Peer reviewed version

Link to published version (if available):
10.1115/SMASIS2017-3829

Link to publication record in Explore Bristol Research
PDF-document

University of Bristol - Explore Bristol Research
General rights

SMASIS2017-3829

DEVELOPMENT OF MULTI-DIMENSIONAL 3D PRINTED VASCULAR NETWORKS FOR SELF-HEALING MATERIALS

Isabel P. S. Qamar
Bristol Interaction Group
Dept. of Computer Science
University of Bristol
Bristol, UK

Richard S. Trask
Dept. of Mechanical Engineering
University of Bath
Bath, UK

ABSTRACT

Self-healing materials have emerged as an alternative solution to the repair of damage in fibre-reinforced composites. Recent developments have largely focused on a vascular approach, due to the ability to transport healing agents over long distances and continually replenish from an external source. However fracture of the vascular network is required to enable the healing agents to infiltrate the crack plane, ceasing its primary function in transporting fluid and preventing the repair of any further damage events. Here we present a novel approach to vascular self-healing through the development and integration of 3D printed, porous, thermoplastic networks into a thermoset matrix. This concept exploits the inherently low surface chemistry of thermoplastic materials, which results in adhesive failure between the thermoplastic network and thermoset matrix on arrival of a propagating crack, thus exposing the radial pores of the network and allowing the healing agents to flow into the damage site. We investigate the potential of two additive manufacturing techniques, fused deposition modeling (FDM) and stereolithography, to fabricate free-standing, self-healing networks. Furthermore, we assess the interaction of a crack with branched network structures under static indentation in order to establish the feasibility of additive manufacture for multi-dimensional 3D printed self-healing networks.

INTRODUCTION

The desire for lighter, more efficient vehicles has resulted in the adoption of fibre-reinforced composites by industries such as automotive and aerospace. However, the damage mechanisms that occur in these materials tend to be extremely complex, leading to structures that are often heavily conservative and overdesigned. In addition, damage detection and repair in composite materials can result in costly maintenance periods. These challenges have been instrumental in the formation of a class of materials that have the ability to self-repair.

To date, self-healing has been demonstrated in bulk polymers [1-10], fibre-reinforced composite laminates [11-22] and sandwich cores [23-24], primarily utilising one of three approaches: intrinsic, microcapsular or vascular. In particular, employing a vascular approach has enabled the continual replenishment of healing agents from an external source and the ability to transport over long distances. However, the potential to heal repeated damage events is limited by the requirement of the vascular network to fracture in order to release the healing agents onto the crack plane, thus terminating its ability to transport fluid to heal subsequent damage. This highlights not only the need for a new approach to the mechanism behind self-healing but also an alternative method for the fabrication of vascular networks, in order to remove the limit on the number of possible healing cycles.

One potential answer lies in Additive Manufacturing (AM), or 3D printing, which is a technology that is revolutionising the way we think about designing and creating objects by enabling highly complex, tailored structures to be fabricated with additional functionality. One example of an advantage this technology can provide to the self-healing community is the ability to create networks that are designed to ensure minimum resistance to flow (such as according to Murray's Law [25]), enabling higher degrees of healing efficiency to be achieved with a reduced time to infusion of more viscous healing agents. The use of extrusion and stereolithographic AM techniques to fabricate 3D vascular networks has previously been reported within tissue

engineering studies [26-34]. However, the application of these technologies to create self-healing vasculature has not yet been extensively explored. By creating a 3D printed network that has the ability to secrete the healing agents without fracture of the network (for example, through a porous wall), successive repeated healing cycles may be entirely possible.

This paper details a new approach to developing self-healing vasculature through an investigation into fused deposition modeling and stereolithography AM techniques and their ability to create free-standing self-healing network structures. An analysis of the quality of the networks and their performance within an embedded fibre-reinforced material subjected to static indentation is undertaken to establish whether they have the required toughness to resist fracture. Furthermore, an experimental study is carried out to assess the flow of healing agents through a 3D printed network and the interaction of a crack with branched network structures is analysed.

SELF-HEALING APPROACH

To overcome the limitations of current microvascular networks, a new concept has been developed that relies on the low surface chemistry of thermoplastic materials and their unwillingness to bond to other materials. This concept is illustrated in Figure 1. By embedding a 3D printed, porous, thermoplastic network into a thermoset matrix, the arrival of a propagating crack to the external wall of the network causes debonding of the network from the matrix, thus exposing the pores and permitting the healing agents to secrete into damage site without fracture of the network. This research focuses on the development of these networks using AM technologies, more specifically extrusion and photopolymerisation based methods. .
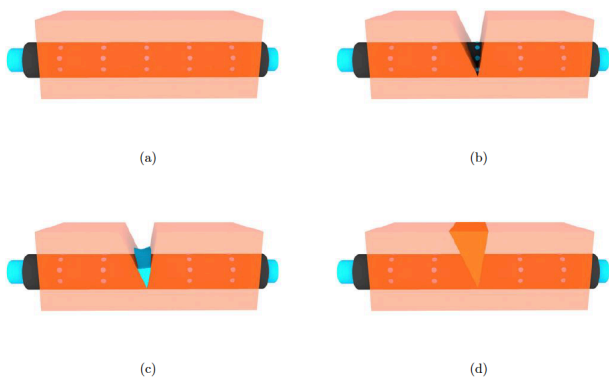

Figure 1 Schematic showing a thermoplastic network embedded within a thermoset matrix that is a) undamaged, b) damaged showing exposed pores, c) damaged with infusion of healing agent, d) healed.

VASCULE FABRICATION

Hollow vascules with an outer diameter of 3.0mm and an inner diameter of 1.4mm (wall thickness twice the nozzle width to promote structural rigidity) were sliced in Cura at a layer height of 0.1mm and printed flat on the print bed using FormFutura Easyfil™ PLA (polylactic acid) with an Ultimaker Original FDM printer. Stereolithographic (SLA) vascules were sliced at a layer height of 0.1mm in PreForm and printed in an automated orientation using a clear acrylic resin with a Formlabs Form1+ printer. Figure 2 displays the vascule cross-sections and Figure 3 a side on view of the vascules. The lower surfaces of FDM vascules were flat where they rested on the print bed and this was necessary to promote adhesion of the vascules to the bed. The uneven cross-section of these vascules can be attributed to the stair-stepping effect of 3D printing techniques that is more pronounced in FDM than other printing technologies. Furthermore, the internal upper surfaces of the FDM vascules had some drooping where the material was unsupported during print, which led to the measured dimension of the inner diameter to be less than that which was input into CAD, as shown in Table 1.
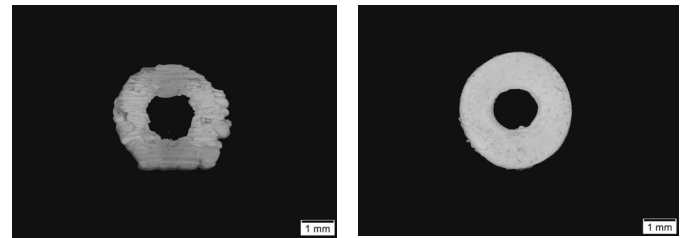

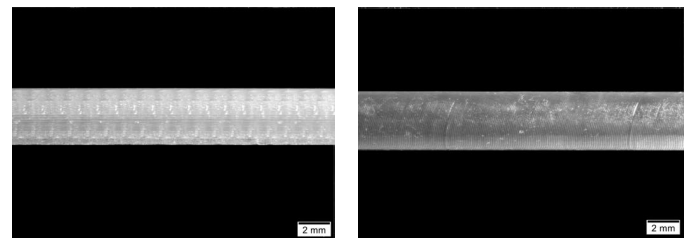**Figure 2 Cross-section of 3D printed vascules printed using FDM (left) and stereolithography (right)**

Figure 3 Side-on view of 3D printed vascules printed using FDM (left) and stereolithography (right)

The stereolithographic vascules remained relatively circular when printed and the 'stair-stepping' was minimal. However, resin often cured within the channel, blocking it and preventing any fluid from flowing through. Table 1 compares the input and output dimensions of the printed vascules, showing that in all cases, the internal diameters were less than the input dimensions and the external diameters were greater. This can be attributed to the aforementioned drooping effect of the FDM vascules and excess resin curing in the case of the SLA vascules.

Table 1 Example Input and measured dimensions for circular vascules printed using FDM (PLA) and stereolithography (SLA) (average of three measurements)

	Internal Diameter (mm)	External diameter (mm)	Wall thickness (mm)
Input	1.400	3.000	0.800
PLA	0.956	3.122	1.057
SLA	0.938	3.163	1.131

CRACK-VASCULE INTERACTION

Vascules with the dimensions listed in Table 1 were embedded at the midline and mid-thickness in both 80 x 80 x 10 mm epoxy (Gurit PRIME™ 20LV) specimens and epoxy specimens with 1 wt% randomly aligned milled carbon fibres (YF International B.V) and cured in an oven for 16 hours at 50°C. The samples were tested under static indentation using a Shimadzu Autograph AG-X machine with a 10kN load cell at a rate of 1mm/min until failure, in order to analyse how a crack interacts with the embedded vascules and whether the vascules remain intact during failure of the host material.

On examining the samples after failure, it was clear that both the PLA vascules and SLA vascules were too brittle to withstand the fracture load and ruptured, terminating their primary role of transporting fluid. The addition of randomly-aligned, discontinuous fibre reinforcement (CF) led to a less catastrophic type of failure, however the vascules still fractured. Figure 4 displays representative load-displacement plots for the different specimen types showing a slight increase in fracture load for samples with fibre reinforcement, however illustrating that the inclusion of vascules did not alter this fracture load. A top view of the indented specimens post-fracture is shown in Figure 5 and micrographs of the crack plane directly below the indentation point showing the fractured vascules are shown in Figure 6.
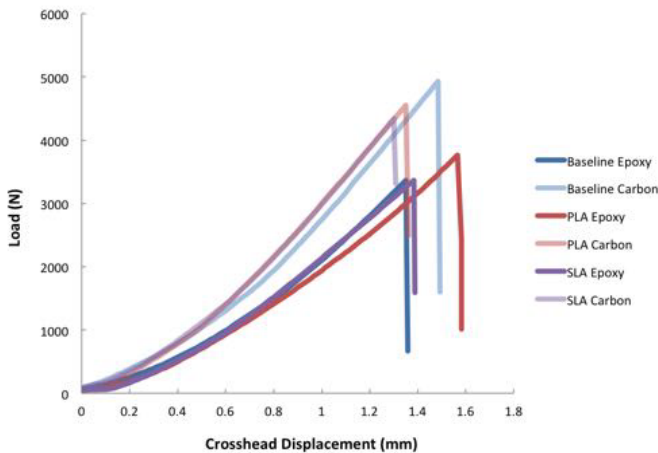

Figure 4 Representative load-displacement plots for baseline, PLA and SLA indentations specimens with and without fibre reinforcement

While it has been determined that both fused deposition modeling and stereolithography are technologies capable of building vasculature, each had their specific advantages and disadvantages which related directly to the creation of self-healing networks. Stereolithography produced vascules of higher quality (i.e. a more even cross-sectional shape and reduced stair-stepping) and the technology could readily create parts in multiple dimensions due to the automatic generation of supports. However, the thin parts tended to warp easily and resin often cured within the internal channels, limiting the minimum attainable vascule bore to 1.4 mm. Furthermore, the compatible materials available for use with this photopolymerisation process are limited and are generally restricted to materials that are more brittle in nature. In comparison, although FDM objects tended to have a higher degree of irregularity in their shape due to stair-stepping and were unable to build complex structures without an additional support material, smaller network bores were achievable (1.0mm) and a high degree of material and process manipulation is possible. Future efforts within this study were therefore placed on enhancing the properties of the vascules produced using an extrusion-based process, however, as materials for 3D printing technologies are being developed at a rapid rate, stereolithography may be worth reconsidering for self-healing vasculature in the future.
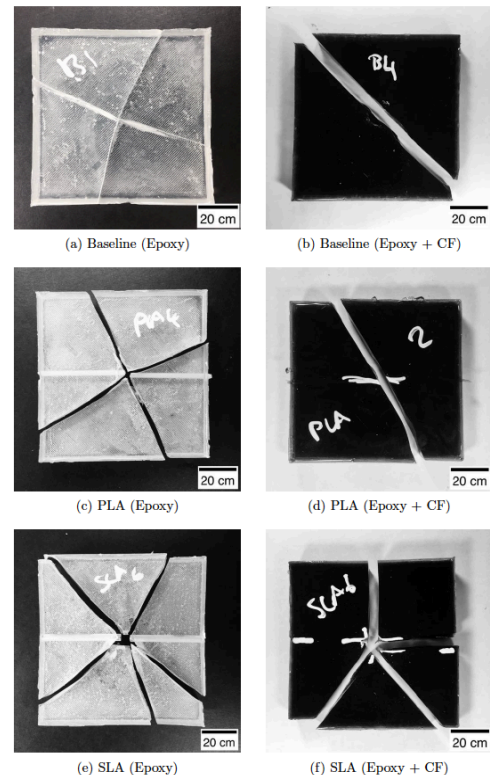

(a) Baseline (Epoxy)

(b) Baseline (Epoxy + CF)

(c) PLA (Epoxy)

(d) PLA (Epoxy + CF)

(e) SLA (Epoxy)

(f) SLA (Epoxy + CF)

Figure 5 Top view of epoxy indented baseline, PLA and SLA specimens with and without carbon fibre reinforcement.

(a) Baseline (Epoxy)

(b) Baseline (Epoxy + CF)

(c) PLA (Epoxy)

(d) PLA (Epoxy + CF)
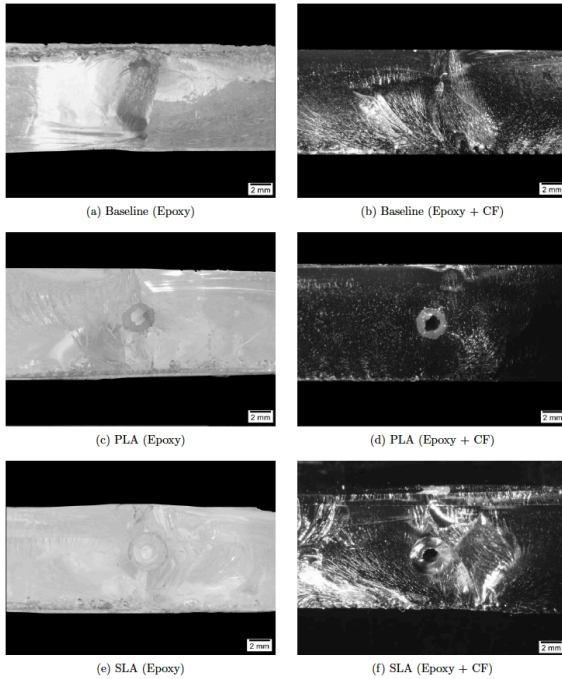
(e) SLA (Epoxy)

(f) SLA (Epoxy + CF)

Figure 6 Crack plane of epoxy indented baseline, PLA and SLA specimens with and without carbon fibre reinforcement, directly below the indentation point.

MATERIALS ANALYSIS

A greater number of filament materials are being developed for compatibility with fused deposition modeling than for any other form of 3D printing, ranging from harder filaments such as PLA and ABS to flexible filaments such as NinjaFlex® (a thermoplastic polyurethane, TPU) and nylon blends. PLA is typically the material of choice for prototype construction, however we have shown that it is incapable of withstanding the loads required to fracture the indentation samples due to its brittle nature, and is therefore unsuitable for self-healing vascule construction. In order to identify a more suitable material, a range of filaments with varying stiffness properties were acquired and tested to establish their quality, mechanical properties (tensile, flexure in three-point bend and fracture toughness) and deformation characteristics under load.

Table 2 lists the properties determined for the selected 'engineering' materials. The data shows that PLA exhibited the highest strengths and stiffnesses of the harder materials tested, however, the more flexible filaments, i.e. Alloy 910 (a nylon-based polymer) and NinjaFlex® had a very high strain to failure and attaining ultimate tensile strengths, flexural strengths and toughness values for these materials was challenging as they deformed rather than broke under load. This emphasised the high resistance of these materials to fracture and suggested that they may be suitable materials for free-standing self-healing vasculature.

However, Alloy 910 suffered from significant water absorption, causing steam bubbles to form in the extruder leading to a rough surface finish. Therefore, the suitability of NinjaFlex® for self-healing vascules was explored.

Table 2 Material properties of FDM filament materials

Material	σ_{UT} (MPa)	E (MPa)	σ_f (MPa)	E_B MPa	K_{Ic} (MPa.m$^{1/2}$)
PLA	55.37	2755	91.65	3432	5.47
PLA/PHA	35.57	1775	88.86	3361	3.99
ColorFabb_XT	34.25	1661	72.68	1861	3.32
ABS	26.60	1601	53.75	1816	2.87
HIPS	9.51	1044	*	1338	1.51
Alloy 910	*	236	*	667	*
NinjaFlex®	*	24	*	31	*

Vascules were printed from NinjaFlex® with an inner diameter of 1.4 mm and an outer diameter of 3.0 mm (for consistency with the PLA and SLA vascules), embedded within epoxy and epoxy with 1 wt% milled carbon fibres and indented in the same procedure as previous. On examining the samples after fracture of the host material, the NinjaFlex vascules remained intact and were exposed to the crack plane in every sample (shown in Figures 7 and 8), identifying itself as a material that is suited to this self-healing approach. Furthermore the vascules cleanly debonded from the surrounding material, whilst bridging the crack and staying within the vascule recess that was created during cure of the host material. Figure 9 displays the representative load-displacement plots.
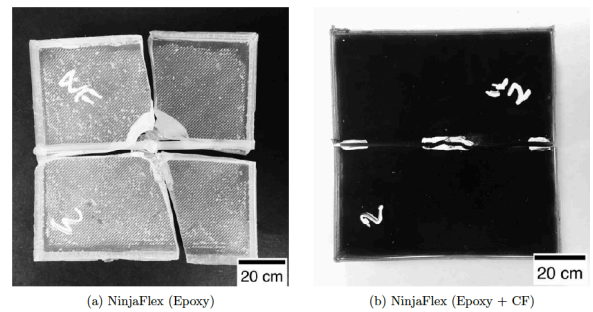

(a) NinjaFlex (Epoxy)

(b) NinjaFlex (Epoxy + CF)

Figure 7 Top view of epoxy indented NinjaFlex specimens with and without carbon fibre reinforcement (white marker fluid indicates placement of vascule).

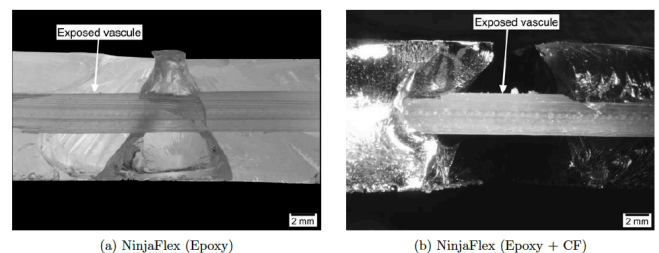(a) NinjaFlex (Epoxy)

(b) NinjaFlex (Epoxy + CF)

Figure 8 Crack plane of epoxy indented NinjaFlex specimens with and without carbon fibre reinforcement, directly below the indentation point.
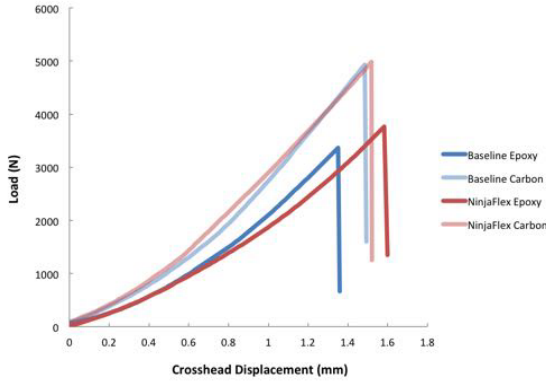
Figure 9 Representative load-displacement plots for baseline and NinjaFlex indentations specimens with and without fibre reinforcement

FLUID FLOW ANALYSIS

To gain an increased understanding of the mechanisms behind fluid flow through a 3D printed network and whether accurate predictions based on the Hagen-Poiseuille equation [35] (Eq. 1) could be achieved, an experiment was undertaken to establish the relationship between the pressure gradient, ΔP (based on static head pressure), and the volumetric flow rate, Q, of a 100cp viscosity (μ) fluid (Silicone oil, Sigma Aldrich) through a straight channel of length (L) 120mm 3D printed from NinjaFlex with the internal diameter dimension, d_i, listed in Table 3.

$$Q = \frac{\pi d_i^4 (\Delta P)}{128 \mu L}$$

(Eq. 1)

Figure 10 displays plots of ΔP vs Q for theoretical predictions based on both the input dimensions into the 3D printer and the measured dimensions output from the 3D printer, and experimental results, highlighting the linear relationship between these two variables. As expected, significant divergence exists between the theoretical predictions based on the CAD dimensions and those determined experimentally, however, there remains good agreement between the theoretical values based on the measured vascule dimensions and those determined experimentally across the range of pressure gradients investigated. This indicates that Poiseuille's Law provides a good approximation for determining the flow rate through 3D printed NinjaFlex networks at the network diameter tested.

Table 3 Input and measured dimensions for circular vascules printed using NinjaFlex via FDM (average of three measurements)

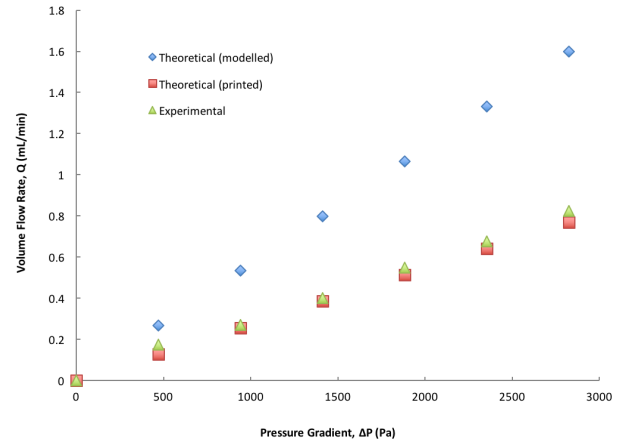|	Internal Diameter (mm)	External diameter (mm)	Wall thickness (mm)
Input	1.400	3.000	0.800
NinjaFlex	1.626	3.009	0.875

Figure 10 Pressure gradient, ΔP, vs volumetric flow rate, Q, for 100cp fluid passing through a 120mm length of NinjaFlex network with a 1.4mm input internal diameter

BRANCHED NETWORK STRUCTURES

Two-dimensional branched network structures, as shown on the left in Figures 11 and 12, were designed and printed to obey Murray's Law [25], with the daughter vessel diameters equal to the one-dimensional vascule diameters previously tested. The networks were embedded within Gurit PRIME™ 20LV resin and hardener with 1 wt% milled carbon fibres and cured for 16 hours and 50°C. Following this, the samples were indented at the centre point (marked by a red X) and the resulting crack patterns examined. Experimental observations noted that when the indentation point was directly above the Y-junction (as in Figure 11), the cracks tended to follow the length of network, however when indented in the centre of a Y branched network between two daughter branches (as in Figure 12), the cracks tended to radiate out from indentation point to the network in three or four locations and cross over the network to the end of the sample rather than following the network. The interaction of the crack with the network is highlighted by the red circles in Figures 11 and 12. These observations suggest that the self-healing mechanism and thus the ease at which the crack plane will be infused depends greatly on the location of the damage initiation point with respect to the network, and that to ensure maximum vascule-damage connectivity and exposure of the network surfaces, the cracks should initiate as close to the network as possible. Although outside the scope of this study, it may be possible to influence the crack path by introducing some degree of fibre alignment within the host material in order to optimise the total length of network exposed to the crack plane for increased healing efficiency.
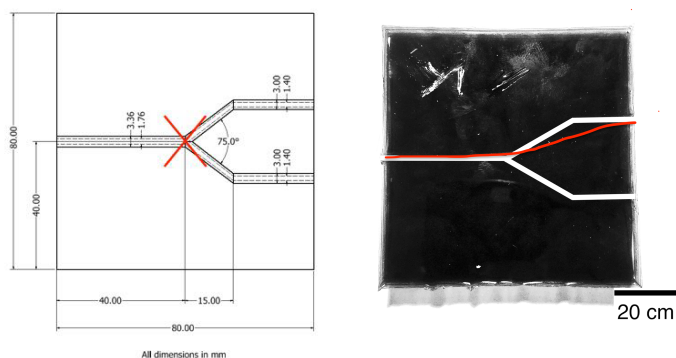
Figure 11 Top view of epoxy indented specimens with and without carbon fibre reinforcement containing a NinjaFlex Y-junction (left - red cross indicated indentation location, right – white lines indicate location of network and red line highlights the crack).
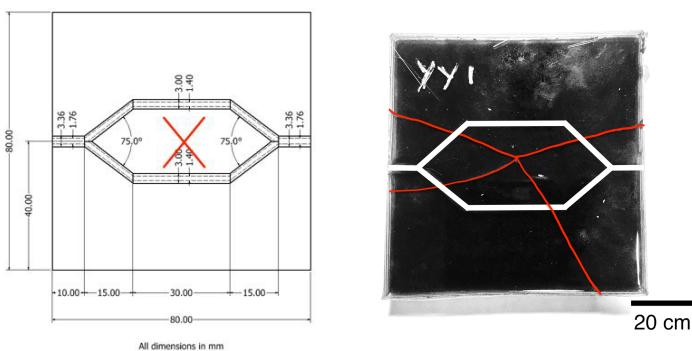

Figure 12 Top view of epoxy indented specimens with and without carbon fibre reinforcement containing a NinjaFlex Y-branched network (left - red cross indicated indentation location, right – white lines indicate location of network and red line highlights the crack).

CONCLUSION

In this paper we investigated the potential of additive manufacturing to fabricate self-healing networks in order to develop a new approach to self-healing, whereby adhesive failure of a porous, thermoplastic network embedded in a thermoset matrix would permit the healing agent to infiltrate the crack plane without fracture of the network. An assessment into two different AM technologies, namely fused deposition modeling and stereolithography, highlighted that, whilst both of these methods were capable of building vasculature, the wide range of compatible filaments available for fused deposition modeling meant that a material could be chosen which would withstand the fracture load of the host matrix. Furthermore, we highlighted the significance in the location of the initiation point with respect to the vascule in ensuring maximum damage-vascule connectivity.

Although these results suggest the suitability of fused deposition modeling and NinjaFlex® for printing self-healing vasculature, questions still surround the ability to include this network methodology into continuous reinforcement, particularly when expanding into multiple dimensions, and the influence of the network on the properties of the host composite material, which, due to the large size of the 3D printed vascules, cannot be considered negligible. Furthermore, expanding these structures into a third dimension will require the use of multi-material deposition, which is still in a relatively experimental phase and requires a material that is suitably compatible with NinjaFlex. However, we have clearly highlighted that potential does exist for 3D printing vascular networks using fused deposition modeling for self-healing materials.

REFERENCES

[1] T. A. Plaisted and S. Nemat-Nasser. Quantitative evaluation of fracture, healing and rehealing of a reversibly cross-linked polymer. Acta Mater., 55:5684–5696, 2007.

[2] J. D. Rule, N. R. Sottos, and S. R. White. E↵ect of microcapsule size on the performance of self-healing polymers. Polymer, 48:3520–3529, 2007.

[3] K. S. Toohey, N. R. Sottos, J. A. Lewis, J. S. Moore, and S. R. White. Self-healing materials with microvascular networks. Nature, 6:581–585, 2007.

[4] D. Therriault, S. R. White, and J. A. Lewis. Chaotic mixing in three-dimensional microvascular networks fabricated by direct-write assembly. Nature, 2:265–271, 2003.

[5] D. Therriault, R. F. Shepherd, S. R. White, and J. A. Lewis. Fugitive inks for direct-write assembly of three-dimensional microvascular networks. Adv. Mater., 17(4):395–399, 2005.

[6] K. S. Toohey, C. J. Hansen, J. A. Lewis, S. R. White, and N. R. Sottos. Delivery of two-part self-healing chemistry via microvascular networks. Adv. Funct. Mater., 19:1399–1405, 2009.

[7] C. J. Hansen, W. Wu, K. S. Toohey, N. R. Sottos, S. R. White, and J. A. Lewis. Self-healing materials with interpenetrating microvascular networks. Adv. Mater., 21:1–5, 2009.

[8] C. J. Hansen, S. R. White, N. R. Sottos, and J. A. Lewis. Accelerated self-healing via ternary interpenetrating microvascular networks. Adv. Funct. Mater., 21:4320–4326, 2011.

[9] A. R. Hamilton, N. R. Sottos, and S. R. White. Self-healing of internal damage in synthetic vascular

materials. Adv. Mater., 22:5159–5163, 2010.

[10] A. R. Hamilton, N. R. Sottos, and S. R. White. Pressurized vascular systems for self-healing materials. J. R. Soc. Interface, 9:1020–1028, 2012.

[11] S. A. Hayes, W. Zhang, M. Branthwaite, and F. R. Jones. Self-healing of damage in fibrereinforced polymer-matrix composites. J. R. Soc. Interface, 4:381–387, 2007.

[12] E. N. Brown, N. R. Sottos, and S. R. White. Fracture testing of a self-healing polymer composite. Exp. Mech., 42:372–379, 2002.

209

[13] E. N. Brown, S. R.White, and N. R. Sottos. Microcapsule induced toughening in a self-healing polymer composite. J. Mater. Sci., 39:1703–1710, 2004.

[14] E. N. Brown, S. R. White, and N. R. Sottos. Retardation and repair of fatigue cracks in a microcapsule toughened epoxy composite: part i: Manual infiltration. Comp. Sci. Tech., 65:2466–2473, 2005.

[15] M. R. Kessler and S. R. White. Self-activated healing of delamination damage in woven composites. Composites: Part A, 32:683–699, 2001.

[16] M. R. Kessler, N. R. Sottos, and S. R. White. Self-healing structural composite materials. Composites: Part A, 34:743–753, 2003.

[17] R. S. Trask and I. P Bond. Biomimetic self-healing of advanced composite structures using hollow glass fibres. Smart Mater. Struct., 15:704–710, 2006.

[18] R. S. Trask, G. J. Williams, and I. P Bond. Bioinspired self-healing of advanced composite structures using hollow glass fibres. J. R. Soc. Interface, 4:363–371, 2007.

[19] C. J. Norris, I. P. Bond, and R. S. Trask. The role of embedded bioinspired vasculature on damage formation in self-healing carbon fibre reinforced composites. Composites Part A, 42:639–648, 2011.

[20] C. J. Norris, I. P. Bond, and R. S. Trask. Interactions between propagating cracks and bioinspired self-healing vascules embedded in glass fibre reinforced composites. Comp. Sci. Tech., 71:847–853, 2011.

[21] C. J. Norris, J. A. P. White, G. McCombe, P. Chatterjee, I. P. Bond, and R. S. Trask. Self-healing fibre reinforced composites via a bioinspired vasculature. Adv. Funct. Mater., 21:3624–3633, 2011.

[22] J. F. Patrick, K. R. Hart, B. P. Krull, C. E. Diesendruck, J. S. Moore, S. R. White, and N. R. Sottos. Continuous self-healing life cycle in vascularized structural composites. Adv. Mater., 26:4302–4308, 2014.

[23] H. R. Williams, R. S. Trask, and I. P. Bond. Self-healing composite sandwich structures. Smart Mater. Struct., 16:1198–1207, 2007.

[24] H. R. Williams, R. S. Trask, and I. P. Bond. Self-healing sandwich panels: Restoration of compressive strength after impact. Comp. Sci. Tech, 68:3171–3177, 2008.

[25] C. D. Murray. The physiological principle of minimum work applied to the angle of branching of arteries. J. Gen. Physiol., 9:835–841, 1926.

[26] S. Engelhardt, E. Hoch, K. Borchers, W. Meyer, H. Krüger, G. Tovar, and A. Gillner. Fabrication of 2D protein microstructures and 3D polymer-protein hybrid microstructures by two-photon polymerization. Biofabrication, 3:025003, 2011.

[27] W. Meyer, S. Engelhardt, E. Novosel, B Elling, M. Wegener, and H. Krüger. Soft polymers for building up small and smallest blood supplying systems by stereolithography. J. Funct. Biomater., 3:257–268, 2012.

[28] M. Schuster, C. Turecek, B. Kaiser, J. Stampfl, R. Liska, and F. Varga. Evaluation of biocompatible photopolymers i: photoreactivity and mechanical properties of reactive diluents. J. Macromol. Sci. Part A, 44:547–557, 2007.

[29] S. Baudis, F. Nehl, S. C. Ligon, A. Nigisch, H. Bergmeister, D. Bernhard, J. Stampfl, and R. Liska. Elastomeric degradable biomaterials by photopolymerization-based CAD-CAM for vascular tissue engineering. Biomed. Mater., 6:055003, 2011.

[30] J. Visser, B. Peters, T. J. Burger, J. Boomstra, W. J. Dhert, F. P. Melchels, and J. Malda. Biofabrication of multi-material anatomically shaped tissue constructs. Biofabrication, 5:1–9, 2013.

[31] A. Skardal, J. Zhang, L. McCoard, X. Xu, S. Oottamasathien, and G. D. Prestwich. Dynamically crosslinked gold nanoparticle-hyaluronan hydrogels. Adv. Mater., 22:4736–4740, 2010.

[32] A. Skardal, J. Zhang, L. McCoard, X. Xu, S. Oottamasathien, and G. D. Prestwich. Photocrosslinkable hyaluronan-gelatin hydrogels for two-step bioprinting. Tissue Eng. Part A, 16:2675–2685, 2010.

[33] A. Skardal, J. Zhang, and G. D. Prestwich. Bioprinting vessel-like constructs using hyaluronan hydrogels crosslinked with tetrahedral polyethylene glycol tetracrylates. Biomaterials, 31:6173–6181, 2010.

[34] Y. Luo, A. Lode, and M. Gelinsky. Direct plotting of three-dimensional hollow fiber sca↵olds based on concentrated alginate pastes for tissue engineering. Adv. Healthcar Mater., 2:777– 783, 2013.

[35] S. P. Sutera. The history of Poiseuille's Law. Annu. Rev. Fluid Mech., 25:1–19, 1993.